



Thermal Analysis Simulation for Laser Butt Welding of Inconel625 Using FEA

Harinadh Vemanaboina^{1*}, G. Edison¹, Suresh Akella², Ramesh Kumar Buddu³

¹SMEC, VIT University, Vellore, Tamilnadu, INDIA

²Sreyas Institute of Engineering & Technology, Hyderabad, INDIA

³Institute for Plasma Research, Gandhinagar, Gujarat, INDIA

*Corresponding author E-mail: vharinadh@outlook.com

Abstract

Laser welding process is employed in the manufacturing of critical components where the final assembly units necessitate strict tolerances like low distortions and residual stresses. Laser beam welding offers several advantages like low heat input, very narrow heat affected zone, low residual stresses, low distortions and good mechanical joint properties in the weld joints when compared to the conventional techniques like Tungsten Inert Gas Arc welding processes. However, the implementation of laser beam welding holds certain challenges like process parameters optimization, experimental set-up and handling and expensive costs. In order to minimize the complex experimental process, simulation techniques using Finite Element Methods (FEM) are employed in order to estimate the heat input and weld process optimization prior to the experiments. This greatly helps in the optimization and estimation of the incurred stresses and distortions with the adapted weld process with known input weld process parameters. The present work reports the Gaussian heat source model for the laser welding of Inconel 625 Alloy plates. The developed moving heat source model is presented and demonstrated with the thermal profiles in terms of the thermal histogram, temperature profiles in the joint cross sections through welded region, interface across the joints.

Keywords: laser welding, moving heat source, Heat flux, FEA, transient thermal analysis.

1. Introduction

Precision welding techniques have gained importance in the manufacturing sector where the components need to be joined with tight final joint tolerances like low distortions and low heat affected zone and good weld joint properties. The typical applications like in the nuclear sector, heat exchangers pressure vessels, space aircraft have explored the laser and electron beam welding techniques to cater the critical demands. Even though these power beam welding processes are very expensive to deal, the final benefits like narrow heat affected zone, low residual stresses and weld quality with good mechanical joint properties like tensile, toughness and fatigue strength kept them as special manufacturing tools for the requirements. Laser welding offers the benefits like low heat input in narrow focus, low distortion and residual stresses, quick production, and ease of tools for weld design. The laser beam welding process parameters optimization of the welded joints is a bit affluent and time-consuming to meet the final product stage manufacturing. During the welding process, the weld thermal behavior controls the weld joint properties like distortions and strength. In order to minimize these issue, the alternative way is to predict the weld joints state using simulation by using the boundary conditions of the weld process parameters in terms of heat input and process conditions. This also provides the 2D and 3D visualization the welded structures using FEM and analysis methods which are widely used. The weld pool temperature state is the initial driving force for changes in residual stress and distortions of the joints in final welded component. Hence, it is important to understand the formation of temperature distributions in

the welded joints like interface, weld zone and through thickness variations. A thermal mapping and isotherms contours will help to estimate the welded structures stress concentration factors and final product conditions.

Inconel alloys are probable candidate materials for high-temperature applications, especially in gas turbine motors, aviation, nuclear applications, because of its fantastic hoisted temperature quality and high corrosion resistance. Inconel is a harder material compared to steels, the temperature distribution from weldments is occurring due to the material contraction during recrystallization process. Thus, homogeneous plastic deformation is generated with distortions and residual stresses compared to the original material as it is cooled [1]. During welding of the plates made of inconel, the sequence of welding plays an important role in distortions that are obtained or Optimizing of distortions can be done by controlling the levels of temperatures and distributions of welding temperature that attained [2]. Harinadh et al [3,4] had established the simulation of similar and dissimilar materials to estimate the distortions and residual stress by simulations using FEM, the stress results are varied in the component due to the change of the heat input for fabricating of the component based on its material thickness and the type of joint [5]. The simulation results show a comparison of different zones of the plate" fusion zone, HAZ, and base plate. Simulation for laser beam welding by Dean Deng [6] had given the SUS316 stainless steel pipe, thermal, distortion, and residual stresses. Komeil Kazemi and John A.Goldak [7] had detailed about the Pecklet number and conductivity of materials for modeling keyhole penetration of laser beam welding, they have modeled a conical profile of keyhole process. Paulo Roberto de Freitas Teixeir [8] used Gaussian distribution for

studying the various heat input for different plate thickness to see their weld pool geometries of the weldments. The sequence of steps for welding process followed in the present work is transient thermal analysis for welding process is shown in Fig.1.

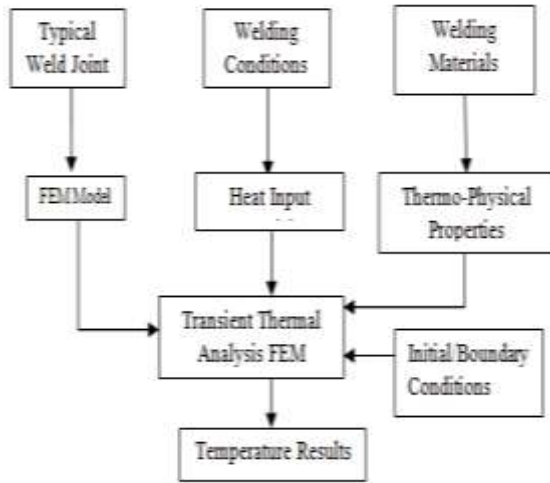


Fig.1: Outline of the transient thermal analysis

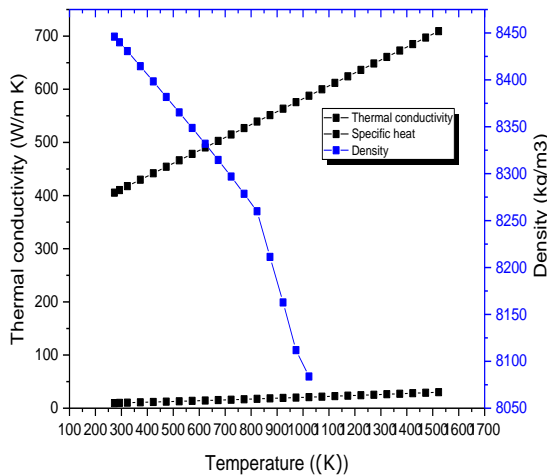


Fig.2: Thermal properties for inconel 625

2. Computational Formulation

The present work is aimed to demonstrate the Inconel plate joining using Laser beam weld process and estimating the temperature profiles under different heat input process conditions and their thermal mapping across the weld and interface zones of the welds. In general laser beam welding show, the Gaussian beam profiles behavior and this is approximately applied in the heat source model selection mostly by a Gaussian heat source models or conical sources with suitable boundary conditions. In the present investigation, a Gaussian heat is modeled to emanate from the laser source. This Gaussian distribution is discretized for modeling in ANSYS. The parametric data language (APDL) in ANSYS is utilized for coding. thermal properties of Inconel consisting of specific heat, density, thermal conductivity are used for the varying temperature obtained during the welding process. The material thermal properties are shown in Fig.2.

The stress is varied in the component due to the change of the heat input for fabricating of the component based on its material thickness and the type of joint. The heat conduction in solid consists of the internal energy, surface heat flux, and the heat conduction is given by Equation (1) Equation (2) is the heat convection from the surface of weld material Equation (3) is the combined heat convection and heat radiation coefficient of the material.

$$c\rho \frac{\partial^2 T}{\partial X^2} = k \left(\frac{\partial^2 T}{\partial X^2} \right) + k \left(\frac{\partial^2 T}{\partial Y^2} \right) + k \left(\frac{\partial^2 T}{\partial Z^2} \right) + Q \quad (1)$$

$$H = 24.1 * 10^{-4} \varepsilon T^{1.61} \quad (2)$$

The heat exchange between the weld material and the ambient happens both as convection and as radiation. The combined effect of these two heat transfer processes is named as a dynamic boundary condition.

$$q_c = H(T - T_0) \quad (3)$$

$$q_r = \varepsilon \sigma (T^4 - T_0^4) \quad (4)$$

Equation 4 is the normal radiation from a surface. $\sigma = 5.67 * 10^{-8} \text{ Wm}^{-2} \text{ C}^{-4}$ defined as the Stefan - Boltzmann constant. Equation (5) is the Gaussian surface flux distribution

$$q(r) = q(0) e^{-cr^2} \quad (5)$$

3. FEM and Heat Source Model

SOLID70 has a three-dimensional warm conduction limit. The segment has eight center points with a lone level of adaptability, temperature, at each center point are shown in Fig.3. The segment is applicable to a three-dimensional, unflinching state or transient warm examination. The segment moreover can compensate for mass transport warm spill out of a relentless speed field. If the model containing the coordinating solid segment is moreover to be analyzed essentially, the part should be supplanted by an equivalent fundamental element. The thermal element meshed with volumetric of a size 0.003.

Welding of nickel-based alloys requires high power for low thick material (150mm X 84 mm X 5 mm), for joining of Inconel 625 the Gaussian distribution surface heat source [9] is used with a radius of 1 mm. A laser beam power of 2 kW and beam speed of 2.83 mm/sec are used in the present modeling. To analyze the welding phenomenon through simulation, a three-dimensional FEM model is developed using ANSYS package as shown in Fig.4 for the transient thermal analysis process. The present model has 4896 number of nodes and 2900 elements.

4. Results and Discussion

In laser beam welding process the final welded joint forms fusion zone and heat affected zone will be less compared to an arc welding process. In a laser beam welding, the maximum temperatures will be at the fusion zone due to the focused narrow beam spot local heating of the material. Fig.6 shows a circle base for the Gaussian normal distribution (bell-shaped curves) at the butt joint of the two plates that are welded. The geometrical parameters of heat flux distribution are estimated from the results of weld simulation. The analyst requires a heat source model that precisely predicts the temperature field in the weldment [10]. A combined convection and radiation boundary condition is used on the remaining of the top surface.

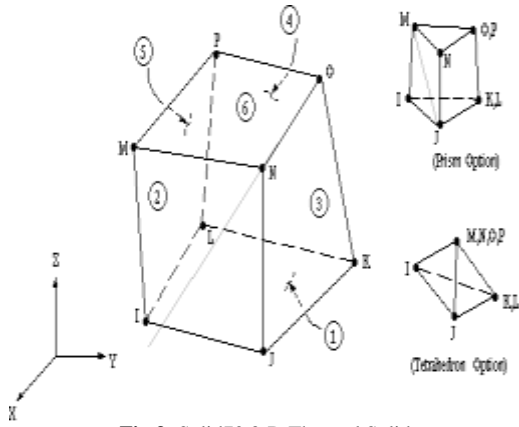


Fig.3: Solid70 3-D Thermal Solid

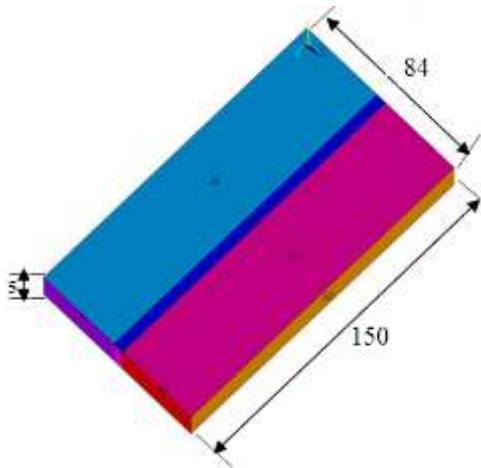


Fig.4: Ansys Model

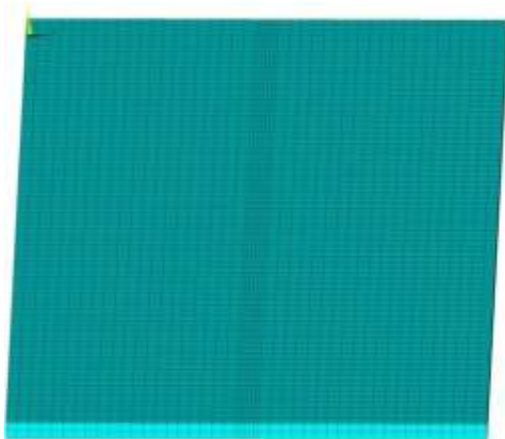


Fig.5: meshing of Ansys Model

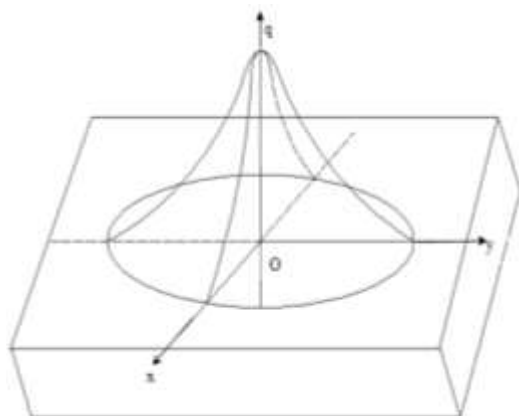


Fig. 6: Gaussian distribution in the mid-surface

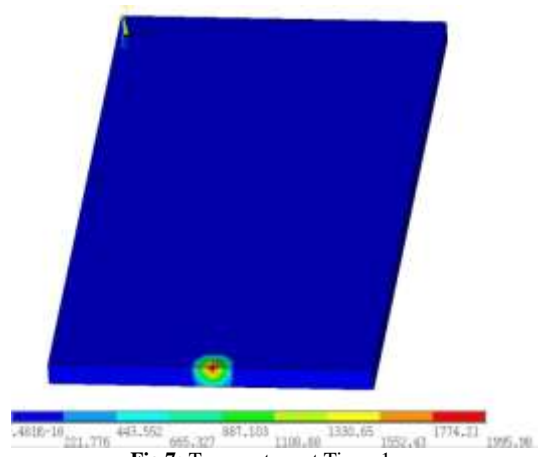


Fig.7: Temperature at Time=1sec

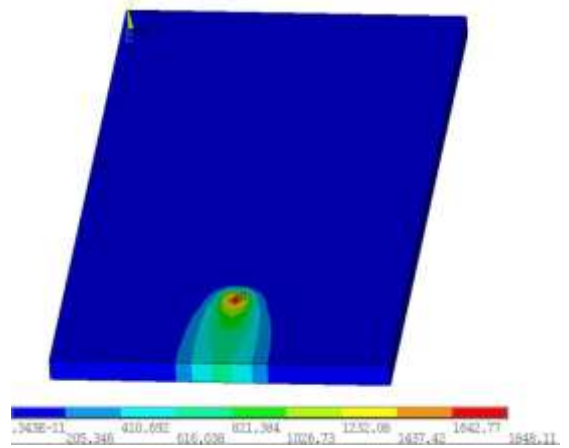


Fig.8: Temperature at Time=10sec

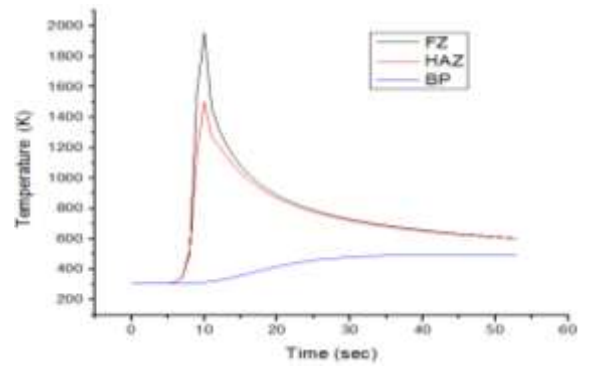


Fig.9: Temperature distributions

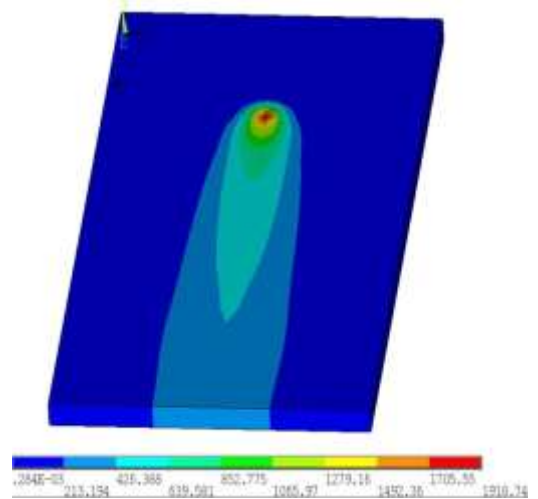


Fig.10: Temperature at Time=35sec

The temperature distribution is shown in the various zone (FZ, HAZ, BP) at equal intervals of time at 1sec, 10sec, 20sec, 30sec, 40sec, 50sec for the present welding simulation temperature profiles are consistent throughout the simulations. At time 1 sec, there is an initial temperature boundary condition and at the 50sec there will be end boundary condition as input conditions. The variations in the temperatures are shown in Fig.15 for the weld zone, HAZ and Base material and clearly show the uniformity in the attained temperatures.

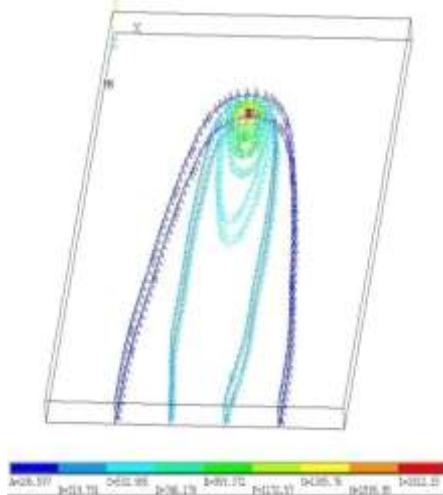


Fig.11: Isotherms of weldments

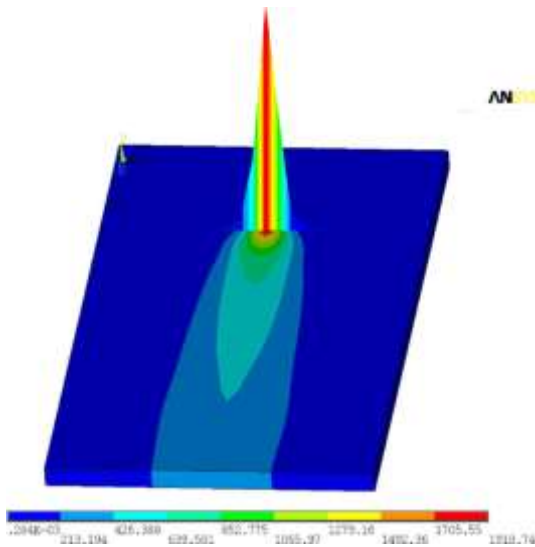


Fig.12: Nodel Temperature of Weldment

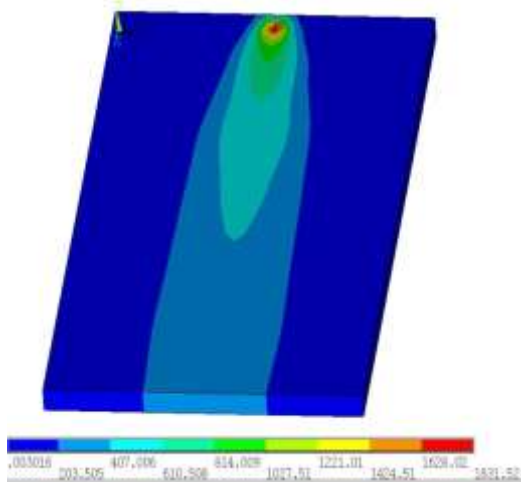


Fig.13: Temperature at Time=50sec

Colour Indication Of The Temperature	Description
	Maximum Temperature Distribution
	Weld Pool Temperature
	Heat Affected Zone
	Less Affected Or Unaffected Zone

Fig.14: Colors indication in the model

In Fig.7 the temperature distribution during the welding process at a time 1sec after the initiation of the weld is shown the temperatures at weld zone is 1995.98°K, it shows that the laser power is concentrated at the weld bead where the joint was built. In Fig.8 the laser beam is moving with respect to time, the maximum temperatures after 10 sec of time are 1848.11°K and minimum is 343°K which is near to ambient temperature. The temperatures of weldment are recorded on the right side of the weldment at FZ, HAZ and the BP in the transverse direction (i.e. perpendicular to weld direction) are shown in Fig.9.

In Fig.10, the temperature distribution of the weld at time 35 sec is shown for details. The temperature distribution is varied from 343°K at the base plate to a maximum of 1919.74°K at the fusion zone during the welding process. Isotherms are plotted at 35 sec to understand the localization of heat condition and also the heat conducted into the plate in transverse, longitudinal and in depth of the weldment for the formation of joints and are shown Fig.11 for detail distribution condition. It is clearly observed that the Gaussian profile of heat distribution weld surface in the in a vertical direction at weld bead surface as shown in the Fig.12 for thermal distribution. It is evident that heat is localized at weld bead is low compared to arc welding processes. The Laser beam moving at constant speed, end of 50 sec the temperature distribution is 1831.52°K are shown Fig.13. The temperature distribution in the weldments are shown with the various color shown in Fig:14 in red indicates high (fusion) and the portion color indicates the heat affected zone and blue color indicates the low temperature (ambient) distribution in the weldment.

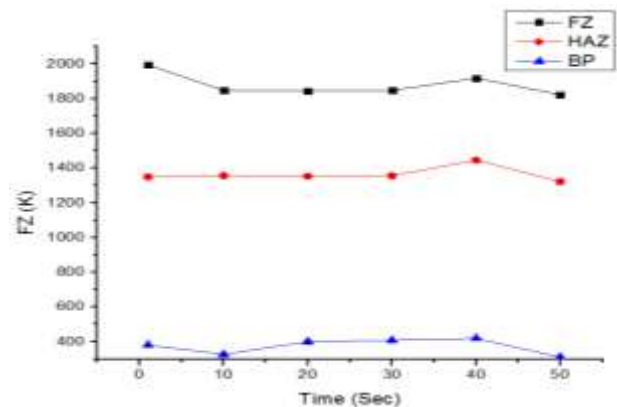


Fig.15: Temperature in transverse direction at various times

5. Conclusions

A moving heat source model for laser beam welding process has been developed with ANSYS FEM simulations and is validated for the weld conditions of 2 KW heat input power for the Inconel 625 material weldability. Different thermal behaviors at the weld zone, Heat Affected zone, and Base materials are evaluated at

different times during the weld process duration. Fusion zone has shown maximum 1900°K and HAZ has shown 1400°K where the Base metal has typical 340°K during the Laser welding with full penetration. A clear indication of uniform thermal behavior is evident in the weldments for given heat input conditions. Dynamic thermal mapping has been generated with the developed moving heat source model is validated. This model is useful for the simulation and comparison of the experimental conditions predictions for the laser welding process.

References

- [1] E. Armentani, et al, (2007)The effect of thermal properties and weld efficiency on residual stresses in welding, journal of Achievements in Materials and Manufacturing Engineering, 20(1),319-322.
- [2] Murakawa, H., Deng, D., Ma, N., & Wang, J. (2012). Applications of inherent strain and interface element to simulation of welding deformation in thin plate structures. Computational Materials Science, 51(1), 43–52. <https://doi:10.1016/j.commatsci.2011.06.040>
- [3] Vemanaboina, H., Akella, S., & Buddu, R. K. (2014). Welding Process Simulation Model for Temperature and Residual Stress Analysis. Procedia Materials Science, 6, 1539–1546. <https://doi:10.1016/j.mspro.2014.07.135>
- [4] Akella,S., Harinadh, V., Krishna, Y., & Buddu R. K. (2014). A Welding Simulation of Dissimilar Materials SS304 and Copper. Procedia Materials Science, 5, 2440–2449. <https://doi:10.1016/j.mspro.2014.07.490>
- [5] Venkatkumar, D., & Ravindran, D. (2016). 3D finite element simulation of temperature distribution, residual stress and distortion on 304 stainless steel plates using GTA welding. Journal of Mechanical Science and Technology, 30(1), 67–76. <https://doi:10.1007/s12206-015-1208-5>
- [6] Deng, D., & Kiyoshima, S. (2010). Numerical simulation of residual stresses induced by laser beam welding in a SUS316 stainless steel pipe with considering initial residual stress influences. Nuclear Engineering and Design, 240(4), 688–696. <https://doi:10.1016/j.nucengdes.2009.11.049>
- [7] Kazemi, K., & Goldak, J. A. (2009). Numerical simulation of laser full penetration welding. Computational Materials Science, 44(3), 841–849. <https://doi:10.1016/j.commatsci.2008.01.002>
- [8] Teixeira, P. R. de F., de Araújo, D. B., & da Cunha, L. A. B. (2014). Study of the gaussian distribution heat source model applied to numerical thermal simulations of TIG welding processes. Ciência & Engenharia, 23(1), 115–122. <https://doi:10.14393/19834071.2014.26140>
- [9] De, A., Maiti, S. K., Walsh, C. A., & Bhadeshia, H. K. D. H. (2003). Finite element simulation of laser spot welding. Science and Technology of Welding and Joining, 8(5), 377–384. <https://doi:10.1179/136217103225005570>
- [10] Karlsson, L., & Goldak, J. (2014). Computational Welding Mechanics. Encyclopedia of Thermal Stresses, 630–637. https://doi:10.1007/978-94-007-2739-7_437